Available online at www.sciencedirect.com
SCIENCE DIRECT®
Tetrahedron: Asymmetry
Tetrahedron: *Asymmetry* 16 (2005) 3084–3093

# Enantioselective preparation and structural and conformational analysis of the chiral solvating agent α,α′-bis(trifluoromethyl)-1,8-anthracenedimethanol

Miriam Pérez-Trujillo,[a] Itziar Maestre,[a] Carlos Jaime,[a] Angel Alvarez-Larena,[b] Juan Francesc Piniella[b] and Albert Virgili[a,*]

[a]*Departament de Química, Universitat Autònoma de Barcelona, E-08193 Bellaterra, Barcelona, Spain*
[b]*Departament de Geologia, Universitat Autònoma de Barcelona, E-08193 Bellaterra, Barcelona, Spain*

Received 18 July 2005; accepted 1 August 2005

Dedicated to Professor J. Castells in the 80th anniversary

**Abstract**—The preparation of the enantiomers of α,α′-bis(trifluoromethyl)-1,8-anthracenedimethanol is described, and their conformational behaviour studied. These enantiomers are very active when used as chiral solvating agents in the presence of several compounds.


## 1. Introduction

The determination of enantiomeric composition by NMR using the addition of a chiral solvating agent (CSA) has been shown[1] to be a valid methodology. After the description of the highly useful[2] Pirkle alcohol,[3] several molecules have been used as CSAs: derivatives of binaphthol[4] or of natural compounds such as quinine[5] and others[6] that form hydrogen bonds or dipolar or π-stacking interactions to generate relatively stable supramolecular entities. Macrocycles, such as calixarenes[7] or cyclodextrins,[8] have also been used as CSAs, with particularly successful results in the aqueous phase. Chiral liquid crystals[9] and gels[10] also afford valuable methods to differentiate enantiomers.

The determination of the absolute configuration by NMR using chiral auxiliaries is better achieved using chiral derivatizing agents.[11] The dynamic character of the association complexes formed using a CSA means that it is difficult to assume only one defined way of association, as well as the absolute configuration. However, some examples have been described.[12] A recent case has been published[13] using Boc-phenylglycine and Kishi proposed[14] the creation of $^{13}C$ NMR databases in chiral solvents.

If a CSA can be used in moderate quantities (1–3 equiv) and if both the substrate and the CSA can be recovered after the analysis, the process of enantiodistinction by NMR is both economical, and practical. We have described[15] the preparation and use of the enantiomers of α,α′-bis(trifluoromethyl)-9,10-anthracenedimethanol **1**, a highly active CSA that separated most of the mixtures of enantiomers assayed[16] (Scheme 1).

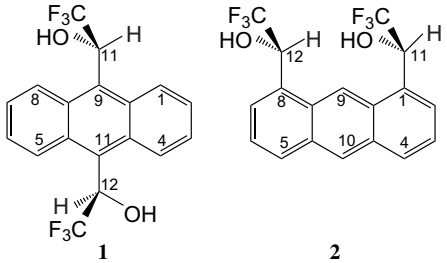


**1** **2**

**Scheme 1.** Structures of (*R*,*R*)-α,α′-bis(trifluoromethyl)-9,10-anthracenedimethanol **1** and (*R*,*R*)-α,α′-bis(trifluoromethyl)-9,10-anthracenedimethanol **2**.

The main factors conferring this capacity are: (i) the presence of two chiral groups containing two highly

* Corresponding author. E-mail: albert.virgili@uab.es

0957-4166/$ - see front matter © 2005 Elsevier Ltd. All rights reserved.
doi:10.1016/j.tetasy.2005.08.005

acidic hydroxyl groups; (ii) the presence of a large aromatic group and (iii) the possibility of a *cisoid* conformation capable of forming two hydrogen bonds with the substrate at the same time. Due to its wide range of application and its capacity to distinguish between enantiomers, compound **1** has been commercialized. Thanks to the relatively acidic character of this compound, it can be used to discriminate substrates with basic functions such as amine groups, carbonyl groups, etc.

We hypothesized that the range of CSAs could be extended by inserting active groups at other positions on anthracene. We thus decided to attempt the synthesis of α,α′-bis(trifluoromethyl)-1,8-anthracenedimethanol **2**, study its structure and examine its inductive chiral properties. This compound conserves the capacity to interact with substrates, forming two hydrogen bonds at the same time. In addition, the accessibility of carbon atom 10 indicates that this compound might have other future applications.

## 2. Results and discussion

### 2.1. Synthesis and resolution

α,α′-Bis(trifluoromethyl)-1,8-anthracenedimethanol **2** was prepared in its enantiopure form and as a mixture of isomers. The two synthetic routes differ only in the last step, the reduction of the prochiral diketone **7** (Scheme 2).

The synthesis was started from 1,8-dichloroanthraquinone **3**. The substitution[17] of chlorine by bromine with KBr gave 1,8-dibromoanthraquinone **4** in 62% yield. Compound **4** was reduced to 1,8-dibromoanthracene **6** by two consecutive reduction–dehydration reactions using $NaBH_4$ as a reducing agent in two different solvents (methanol and diglyme). This process has only been described for chloro- and iodoanthraquinones.[18] The first reaction gave 4,5-dibromo-9-anthrone **5** (68% yield), which was isolated and characterized, while the second reaction gave compound **6**, 1,8-dibromoanthracene,[19] in 69.5% yield from quinone **4**. Alternatively, the complete reduction of **4** to **6** was also carried out after nine days of reaction (71% yield) with a great excess of aluminium *sec*-butoxide.[20]

By extension of the methodology previously applied,[21] the generation of the dilithium derivative from butyl lithium and the subsequent reaction with trifluoroacetic anhydride yielded 1,8-trifluoroacetylanthracene **7** (52%). This intermediate product **7**, was isolated and characterized by NMR. 1-Trifluoroacetylanthracene **8** was detected and isolated as a sub-product of the reaction.

Compound **7** was reduced with $NaBH_4$, giving a mixture of diastereoisomers: *meso*-**2** and racemic (*R*,*R*)-**2** and (*S*,*S*)-**2** in moderate yield (52%). The enantioselective reduction of diketone **7** was carried out by the asymmetric CBS[22] reduction, as recently applied to the reduction of 1,8-trifluoroacetylanthracene in the direct preparation of the enantiomers of **1**.[23] In this way, the reduction of **7** using catecholborane and (*S*)-oxazaborolidine gave

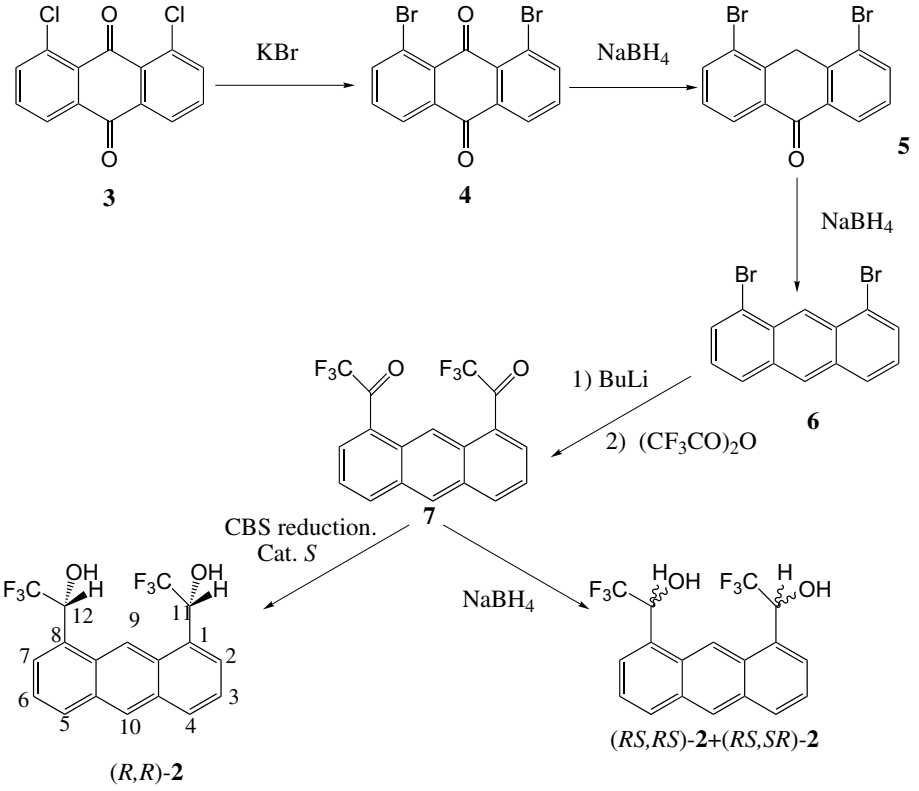


**Scheme 2.** Synthesis of alcohol **2**.

(*R*,*R*)-α,α′-bis(trifluoromethyl)-1,8-anthracenedimethanol **2** in 89% yield, with only 1.7% of *meso*-**2** compound, which could have been separated by flash chromatography.

The enantiomeric composition was always established by preparation of diacetate derivatives **9** that were separated by analytical chiral HPLC. The selectivity was 97%.

The diacetate derivative of racemic **2**, compound **9**, was prepared quantitatively by treatment with acetyl chloride and used to isolate pure enantiomers by HPLC on a semi-preparative Whelk-O2 chiral column using hexane/isopropyl alcohol (98:2) as the eluting solvent (3 mL/min). The first compound eluted was (−)-**9** (the (*R*,*R*)-**9** as described below); the second compound was the optically inactive *meso*-**9** and the third was (+)-**9** [(*S*,*S*)-**9**]. Their hydrolysis yielded the corresponding pure enantiomers (−)-(*R*,*R*)-**2** and (+)-(*S*,*S*)-**2**, respectively. The direct formation of the diacetates prepared from each pure enantiomer obtained by the enantioselective reduction of diketone **7**, (−)-(*R*,*R*)-**2** and (+)-(*S*,*S*)-**2**, also gave the diacetates (−)-(*R*,*R*)-**9** and (+)-(*S*,*S*)-**9**, respectively.

### 2.2. Structural study

The crystal structure of (−)-(*R*,*R*)-**2** was studied by X-ray.[24] Suitable crystals were obtained from an ether solution (Fig. 1). In the solid state, the molecule adopts an asymmetrical conformation. On one side the $CF_3$ group defines a torsion angle of nearly 90° [C2–C1–C11–C21, 94.9(6)°], and on the other side the OH substitute is closest to an almost orthogonal plain to the aromatic ring [C7–C8–C12–O22, −98.8(6)°]. In this case, one of the fluorine atoms of the trifluoromethyl group forms a hydrogen bond with the hydroxyl group on the same stereogenic centre.

Molecules are linked by O–H···O hydrogen bonds forming infinite chains, in which each oxygen atom acts as donor and acceptor. Hence, every molecule is linked to four neighbours (Fig. 1). Moreover, one of the O–H···O participates in a three-centre hydrogen bond where an intramolecular O–H···F is present. Geometric data of hydrogen bonds are:

O21H21···O22i: O21–H21, 0.82 Å; H21···O22i, 2.00 Å; O21···O22i, 2.753(6) Å; O21–H21···O22i, 152°. i: $x+1$, $y$, $z$.

F6···O22H22···O21ii: O22–H22, 0.82 Å; H22···O21ii, 2.20 Å; O22···O21ii, 2.882(6) Å; O22–H22···O21ii, 141°; H22···F6, 2.37 Å; O22···F6, 2.780(6) Å; O22–H22···F6, 112°; O21···H22···F6, 107°. ii: $x-1$, $-y+1$, $-z+1$.

Overlapping of the outside aromatic rings of anthracene provides additional stabilization to infinite chains by π-interaction. Two stacks of parallel molecules can be observed in every chain (Fig. 1) with a distance of 3.59 Å between two adjacent parallel molecules. Polar groups (and the network hydrogen bonds) lie between the two stacks, in the middle of the chain.

The asymmetry observed in the solid phase was not seen in the liquid phase. The $^1$H NMR ($CDCl_3$) spectrum affords only seven signals, indicating the kinetic equivalence of protons $H_2/H_7$, $H_3/H_6$, $H_4/H_5$ and $H_{11}/H_{12}$. Moreover, no changes were observed in the spectrum at low temperature (220 K), indicating a rapid rotation of the $C_1$–$C_{11}$ and $C_8$–$C_{12}$ bonds. The NOE experiment (Fig. 2) of (*R*,*R*)-**2** with saturation of $H_{11}/H_{12}$ revealed a high increase of the intensity of $H_9$ and a very low increase on $H_2/H_7$, indicating the principal proximity of $H_{11}/H_{12}$ with $H_9$.

The theoretical study of its conformational behaviour started with a Monte-Carlo search (MacroModel package,[25] using the AMBER* force field[26]). All conformers were obtained by rotation around the two $sp^2$–$sp^3$ bonds ($C_1$–$C_{11}$ and $C_8$–$C_{12}$) and the two C–OH bonds, giving a total of 272 structures. Four sets of conformers were identified by the rotation around the $sp^2$–$sp^3$ bonds. These sets will subsequently be referred to as follows: *trans1* (T1), *cis* (C), *crystal* (X) and *trans2* (T2) (Fig. 3). Each set contained several rotamers around

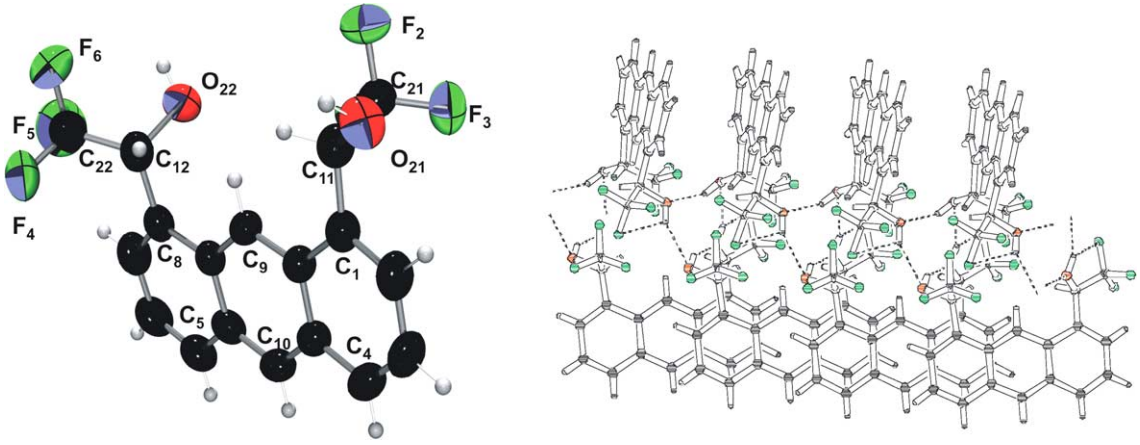


**Figure 1.** X-ray structure of (−)-(*R*,*R*)-**2**.

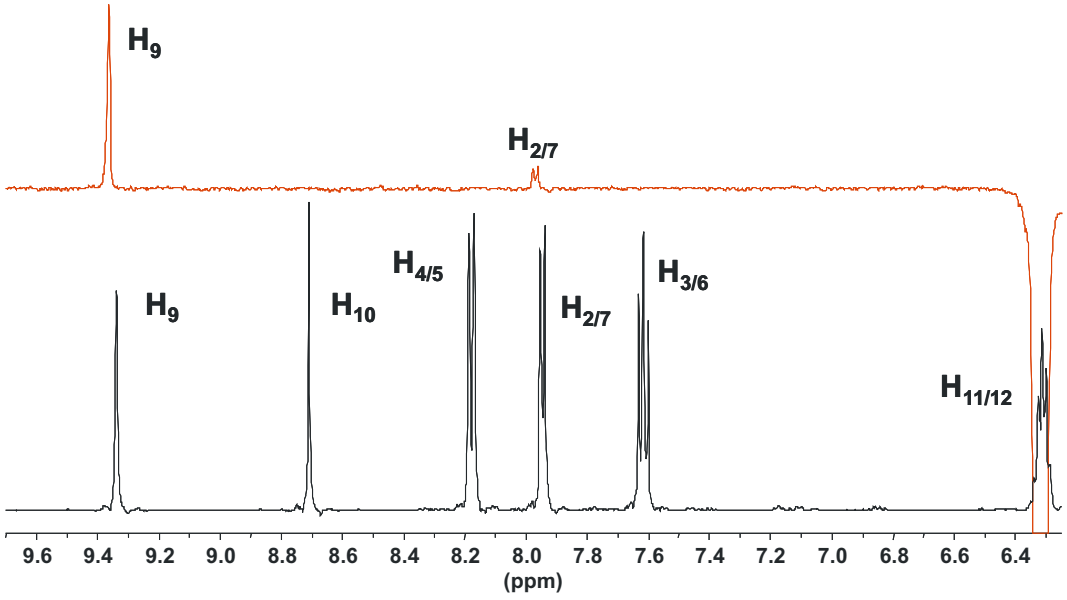


**Figure 2.** $^1$H NMR ($CDCl_3$) spectrum of (*R*,*R*)-**2** and 1D DPFGNOE spectrum after saturation $H_{11/12}$.

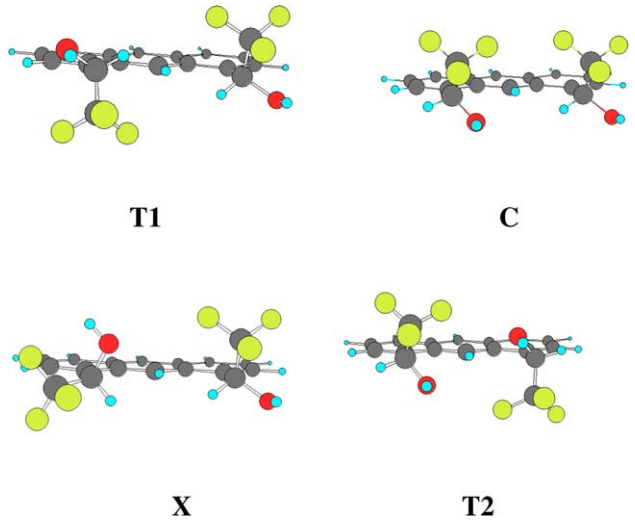


**Figure 3.** Representative structures for each conformer set: T1 = *trans1*; C = *cis*; X = crystal; T2 = *trans2*.

the C–OH bonds. Relative energies obtained for the T1, C, X and T2 conformers (0.0, 2.9, 6.2 and 8.89 kJ/mol, respectively), suggest that T1 is the most stable, followed by C (computed populations based on Boltzmann's distribution were 71.6%, 20.5%, 5.9% and 2.0%, respectively).

T1 and T2 conformers have a $C_2$-symmetry axis and the $CF_3$ groups are located in a *transoid* position. In the C conformer, the *cisoid* distribution of the substituents substitutes is asymmetric, while the X conformer is very similar to the X-ray structure. Moreover, T1 is the most stable and the distance between $H_9$ and $H_{11}/H_{12}$ (about 2 Å) is consistent with the NOE obtained in $CDCl_3$ shown in Figure 2. The low proportion of the *cisoid* (C) conformer may thus be responsible for the other small NOE observed (Fig. 2) between $H_{11}/H_{12}$ and $H_2/H_7$.

The energy surface corresponding to the rotation of the two $sp^2$–$sp^3$ bonds (i.e., the conversion between the *transoid* and the *cisoid* conformers) was obtained using the dihedral angle driver implemented into the Macromodel (Fig. 4).

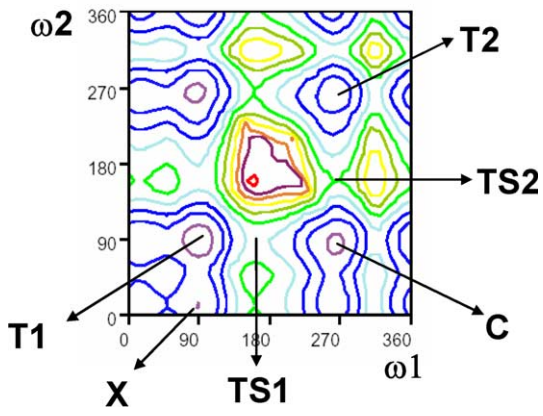


**Figure 4.** Contour plot for the potential energy (kJ/mol) surface corresponding to the rotation of the $C_1$–$C_{11}$ ($\omega$1) and $C_8$–$C_{12}$ ($\omega$2) bonds.

The transition from T1 to T2 must pass through C. Conformer X is very close in geometry to T1. The transition state (TS1) between T1 and C is about 5 kJ/mol less energetic than that (TS2) between C and T2. The overall energy barrier for the free rotation around the $sp^2$–$sp^3$ bonds is about 54 kJ/mol.

**2.2.1. Chiral induction activity.** The behaviour of **2** as a chiral solvating agent was tested with five racemic mixtures: 1-(1-naphthyl)ethylamine **10**, 1-aminoindane **11**, 1-*cis*-amino-2-indanol **12** and phenylethanediol **13** and 1-phenylethylamine **14** (Scheme 3). Both enantiomers of **2** were used, but as the behaviour of the two

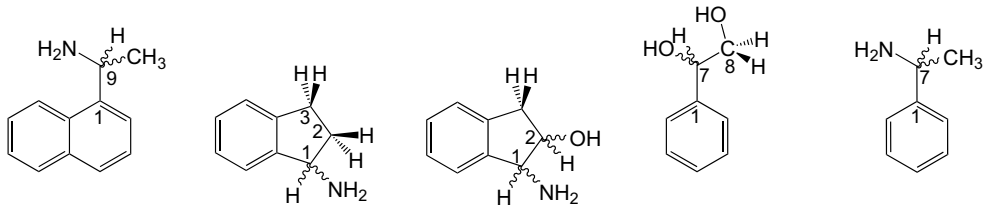


**Scheme 3.** Compounds evaluated in the enantiodiscrimination tests.

enantiomers in the presence of the same racemic compound is symmetrical the results are always referred to those obtained with the (*R*,*R*)-**2** enantiomer.

In all cases the experiments were carried out by adding portions of CSA to a solution (0.05 M) of the racemic substrate until a maximum increase of non-equivalence was obtained (2–2.5 equiv). The signals of each enantiomer were identified using mixtures enriched in one of the enantiomers of a known composition. The enantiomeric identity was based on the integration of the separated signals.

The enantiodifferentiation will be shown in three ways: the variation of the spectra by the addition of variable quantities of CSA, the graphic illustration of the values of the difference obtained or giving the maximum separation obtained between the enantiomers.

Figure 5 shows experiments corresponding to compounds **10** and **11** where the enantiodistinction was plotted in front of the molar relation between the components. The additional curves show the tendency for a maximum enantiodistinction for each proton measured. The differences observed between the chemical shift of the enantiomers using (*R*,*R*)-**2** were quantitatively similar to those found[15] using (*R*,*R*)-**1**, but (*R*,*R*)-**2** also enantiodifferentiates nuclei not separated by (*R*,*R*)-**1**, for example, the signals of $H_1$ of **11**, $CH_3$ of **10** and $H_2$ in **12**.

The obtained spectra for compounds **12** and **13** are represented in Figures 6 and 7 where one can observe the variation of the enantiodistinction by the addition of several quantities of the CSA (*R*,*R*)-**2**. The action on compound **13** is more selective, while (*R*,*R*)-**1** differentiated the $H_1$ of their enantiomers, (*R*,*R*)-**2** distinguished the $H_2$.

For each substrate, the maximum enantiodistinction was obtained with different quantities of CSA. Table 1 shows the greatest difference of chemical shift of $^1$H NMR obtained for several protons of compounds **10**–**14** when some quantities of (*R*,*R*)-**2** were added. In all cases, the separation was enough to integrate separately both enantiomers.

The study of the association complexes was carried out with substrates **10** and **12**. The stoichiometry was checked using the Job plot,[27] indicating a 1:1 composition of both binding complex.

Binding constants[28] were measured in $CDCl_3$ by the equimolecular method,[29,30] which is based on the results obtained with several solutions of identical relative concentrations[31] of the components that form a 1:1 association. Under these conditions, the variation of the chemical shifts ($\Delta\delta$) analyzed as a function of the $(\Delta\delta/S_0)^{1/2}$ ($S_0$ = concentration) results in a linear relation $[\Delta\delta = -(\delta_c/K)^{1/2}(\Delta\delta/S_0)^{1/2}]$ ($\delta_c$ = chemical shift of pure complex).[32] To avoid competitive processes, we used each pure enantiomer in separate experiments.

Tables 2 and 3 show the equilibrium constants obtained for the association of (*R*)-**10** and (*S*)-**10** with (*R*,*R*)-**2** and for the association of (*R*,*S*)-**12** and (*S*,*R*)-**12** with (*R*,*R*)-**2** at four temperatures. The values of *K* and Gibb's energy are slightly lower than those obtained[15] for (*R*,*R*)-**1**. The difference between the enantiomers increases at lower temperature.

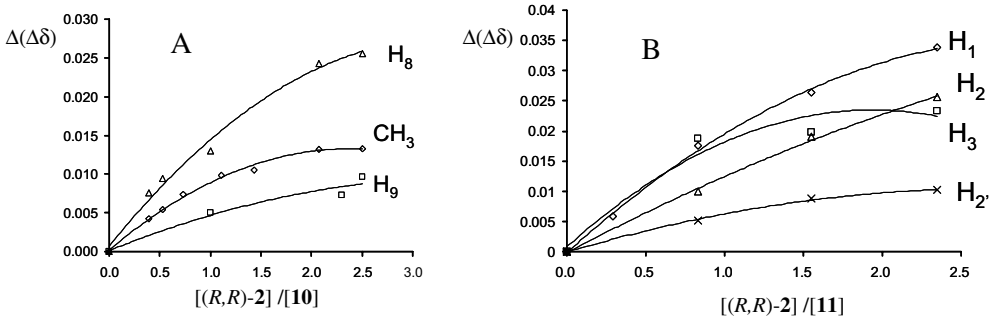


**Figure 5.** Evolution of the enantiodifferentiation at 300 K of several protons of **10** (A) and **11** (B) (0.05 M in $CDCl_3$) when several portions of CSA were added at a range of molar ratios.

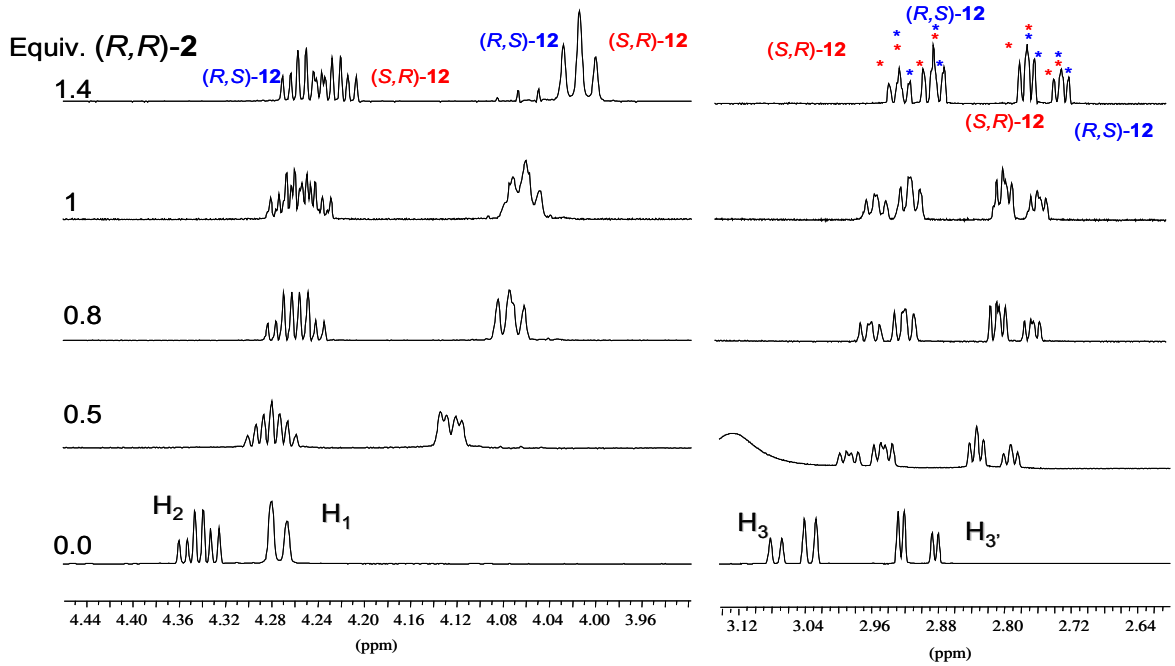


**Figure 6.** Enantiodifferentiation of 1-*cis*-amino-2-indanol **12** after the addition of several quantities of (*R*,*R*)-**2**.

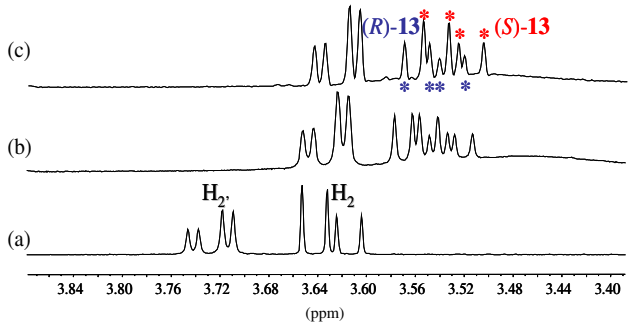


**Figure 7.** Enantiodifferentiation of phenylethanediol **13** using (*R*,*R*)-**2**: (a) compound **3** pure; (b) addition of 1 equiv of (*R*,*R*)-**2** to racemic **3**; (c) addition of 1 equiv of (*R*,*R*)-**2** to a mixture 1.5/1 enriched in the enantiomer (*S*)-**13**.

**Table 1.** Maximum difference ($\Delta(\Delta\delta)$) between the enantiomers of **10**–**14** obtained when (*R*,*R*)-**2** is added

| Substrate + (equiv) of (*R*,*R*)-**2** | Proton | $\Delta(\Delta\delta)$/ppm |
|---|---|---|
| **10** + (2 equiv) | $H_3$ | 0.030 |
| | $H_8$ | 0.024 |
| | $H_9$ | 0.007 |
| | $CH_3$ | 0.013 |
| **11** + (2.3 equiv) | $H_1$ | 0.034 |
| | $H_2$ | 0.028 |
| | $H_{2'}$ | 0.010 |
| | $H_3$ | 0.021 |
| **12** + (1.4 equiv) | $H_1$ | 0.014 |
| | $H_2$ | 0.030 |
| | $H_3$ | 0.013 |
| | $H_{3'}$ | 0.011 |
| **13** + (1.5 equiv) | $H_2$ | 0.015 |
| **14** + (2.4 equiv) | $H_7$ | 0.007 |
| | $CH_3$ | 0.009 |

**Table 2.** Equilibrium constants (±SD) of the complexes formed between the enantiomers of **10** with (*R*,*R*)-**2**, measured by the equimolecular method (in $CDCl_3$)

| *T*/K | (*R*)-**10** | | (*S*)-**10** | |
|---|---|---|---|---|
| | $K_R/M^{-1}$ | $\Delta G^\circ_R$/kJ/mol | $K_S/M^{-1}$ | $\Delta G^\circ_S$/kJ/mol |
| 255 | 59 ± 9 | −8.6 ± 0.3 | 102 ± 6 | −9.8 ± 0.1 |
| 270 | 51 ± 8 | −8.8 ± 0.3 | 58 ± 4 | −9.1 ± 0.2 |
| 285 | 18 ± 4 | −6.9 ± 0.5 | 26 ± 1 | −7.7 ± 0.1 |
| 300 | 14 ± 2 | −6.6 ± 0.4 | 22 ± 1 | −7.7 ± 0.1 |

**Table 3.** Equilibrium constants (±SD) of the complexes formed between the enantiomers of **12** with (*R*,*R*)-**2**, measured by the equimolecular method (in $CDCl_3$)

| *T*/K | (*R*,*S*)-**12** | | (*S*,*R*)-**12** | |
|---|---|---|---|---|
| | $K_{RS}/M^{-1}$ | $\Delta G^\circ_{RS}$/kJ/mol | $K_{SR}/M^{-1}$ | $\Delta G^\circ_{SR}$/kJ/mol |
| 255 | 30 ± 2 | −8.5 ± 0.3 | 113 ± 35 | −10.0 ± 1.3 |
| 270 | 19 ± 3 | −7.3 ± 0.8 | 69 ± 2 | −7.8 ± 0.2 |
| 285 | 19 ± 5 | −7.3 ± 1.2 | 23 ± 1 | −10.6 ± 0.2 |
| 298 | 6 ± 1 | −4.6 ± 0.1 | 9 ± 1 | −11.8 ± 0.2 |

Since the differences between the constants of each pair of enantiomers are small, the greater enantiodifferentiation observed when (*R*,*R*)-**2** is used may be attributed to the differences in the geometry of the complexes rather than the differences of displacement of the equilibrium. The thermodynamic factor seems to influence the separation of the enantiomers only at low temperatures.

The $^1H$ NMR spectrum of **10** with (*R*,*R*)-**2** shows all the signals shifted upfield. Although $H_9$ and $CH_3$ of **10** are shielded, the $H_9$ of (*S*)-**10** is more shielded than that of (*R*)-**10** and, furthermore, the $CH_3$ of (*S*)-**10** is less shielded than that of (*R*)-**10**. Therefore, $H_9$ and $CH_3$

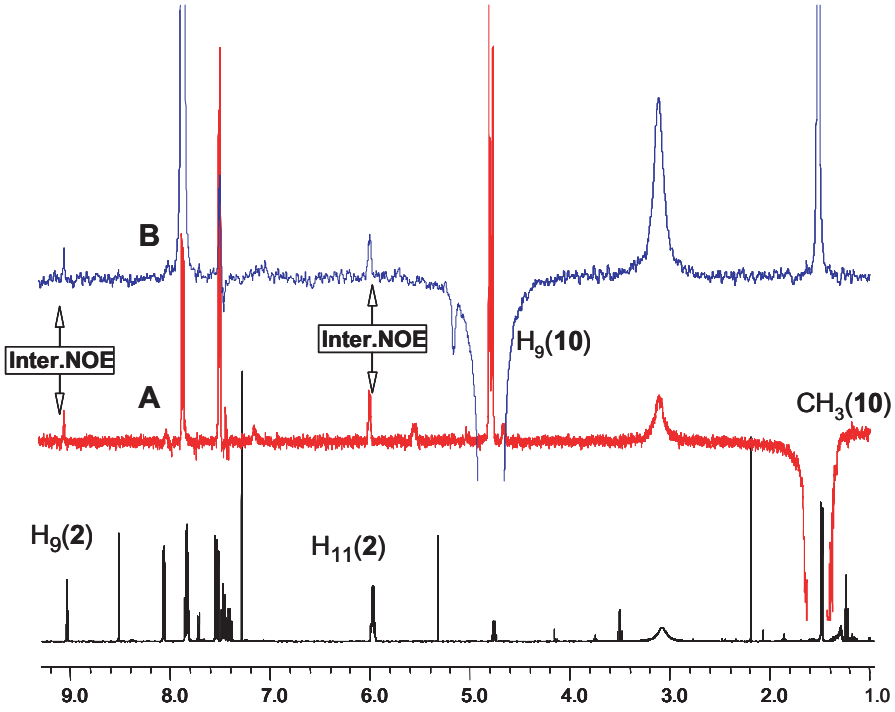


**Figure 8.** 1D NOE spectra of the association (in $CDCl_3$) between (*R*,*R*)-**2** and *S*-**10** after saturation of $CH_3$ (A) and $H_9$ (B) of compound **10**. The spectra were obtained using the 1D DPFGNOE sequence at 300 K.

of the enantiomers of **10** show an opposite behaviour in the presence of (*R*,*R*)-**2**. The diastereomeric complexes of (*R*,*R*)-**2** with amine **10** were studied by NOE spectra and obtained (Fig. 8) via gradient selection DPFGNOE.[33]

Figure 8 presents the NOE spectra of complex [(*R*,*R*)-**2**·(*S*)-**10**] when $H_9$ and $CH_3$ of the amine **10** were saturated, obtaining intermolecular NOE on $H_9$ and $H_{11}$ of the alcohol **2**. The opposite experiment, that is, the saturation of $H_9$ and $H_{11}$ of the (*R*,*R*)-**2**, gives the same results.

The complex [(*R*,*R*)-**2**·(*R*)-**10**] gave similar NOE results, so it was impossible to differentiate the complexes on the basis of NOE information. The presence of NOE indicates a closeness between the atoms of two components confirming the formation of the complex.

## 3. Conclusion

We can conclude that there are stereochemical differences dependent on whether the substrate binds to (*R*,*R*)-**1** or (*R*,*R*)-**2**, which indicates that their use in combination would enable us to differentiate a wide range of the substrates.

## 4. Computational details

The Monte-Carlo search was performed with the appropriate options in the Macromodel v.5 program[25] with an AMBER* force field.[26] A total of 1000 steps were allowed and the search was performed by randomly changing the $C(sp^2)$–$C(sp^3)$ and $C(sp^3)$–O dihedral angles between 0° and 360°. The conformers obtained (272) were distributed into four groups (see text) on the basis of the relative positions of the trifluoromethyl groups. A potential energy surface corresponding to the simultaneous movement of both $C(sp^2)$–$C(sp^3)$ bonds was also computed with the AMBER* force field.

## 5. Experimental

NMR spectra were recorded at 400.13 and 500.13 MHz for $^1H$. The temperature was controlled to 0.1 °C. The NMR signals were identified from several 1D (DEPT, NOE) and 2D (COSY, HMQC and HMBC) spectra.

The experiments of enantiodiscrimination by NMR were carried out with 0.5 mL of a solution 0.05 M ($CDCl_3$) of the tested compounds **10** to **14**. After addition (at constant volume) of several portions of 0.2–0.5 equiv of CSA (*R*,*R*)-**2**, $^1H$ NMR spectra were measured and the variations of the chemical shifts were calculated for each addition. The measurements were continued until maximum enantiodiscrimination (1.5–2.5 equiv) or until precipitation. The NOE experiments on amine **10** complexes were performed on degassed samples using DPFGNOE sequence with a 700 ms mixing time.

The equimolar method was applied (at four temperatures) to 0.5 mL of a solution ($CDCl_3$) of each enantiomer of the substrate **10** or **12** with the CSA (*R*,*R*)-**2** at identical concentrations (0.05 M each) and the $^1H$

NMR obtained. New values of the chemical shift were measured after the addition of 0.1 mL of pure solvent, four times. A straight line (and the corresponding standard deviation) was obtained after the representation ($\Delta\delta$ in front of $(\Delta\delta/S^{\circ})^{1/2}$) of Bouquant and Chuche's equation. The binding constant $K$ was obtained from the slope ($((\delta_c/K)^{1/2}$) and the chemical shift of the hypothetically pure association complex ($\delta_c$) from the intersection of the straight line with the $Y$-axis. The final value of $K$ was obtained from the averaged value of those obtained for each proton measured.

Chiral semi-preparative HPLC was carried out using an (*R*,*R*)-Whelk-O1 (250 mm × 10 mm) column and preparative HPLC using an (*R*,*R*)-Whelk-O2 (250 mm × 25 mm) column.

### 5.1. 1,8-Dibromoanthraquinone 4

1,8-Dichloroanthraquinone **3** (10 g, 36.10 mmol) was treated with KBr (20 g, 168.05 mmol), $CuCl_2$ (0.5 g, 3.72 mmol) and 85% $H_3PO_4$ (20 mL) in nitrobenzene (75 mL). Water was distilled from the reaction mixture until the temperature reached 200 °C. Then the mixture was refluxed for 48 h. The crude was precipitated from the cooled mixture with methanol, collected, taken up in $CH_2Cl_2$ and isolated by evaporation of the solvent. Purification of the solid residue by crystallization in hot nitrobenzene yielded 10.1 g of a 5:4:1 mixture (estimated by GC–MS) of **4**, 1-bromo-8-chloroanthraquinone and compound **3**, as golden needles. The same procedure was repeated using the last mixture as starting material and refluxing for 24 h, to give 8.2 g of **4** (62%). Mp: 152–154 °C. IR $\nu = 3063$, 1679, 1659, 1570, 1311, 1238 $cm^{-1}$. $^1H$ NMR (500 MHz, $CDCl_3$, 298 K): $\delta = 7.53$ (dd, $J = 7.9$ Hz, $J = 7.9$ Hz, 2H, $H_3$ and $H_6$), 8.01 (dd, $J = 8.0$ Hz, $J = 1.3$ Hz, 2H, $H_2$ and $H_7$), 8.23 (dd, $J = 7.8$ Hz, $J = 1.2$ Hz, 2H, $H_4$ and $H_5$). $^{13}C$ NMR (125 MHz, $CDCl_3$, 298 K): $\delta = 122.1$ ($C_1$ and $C_8$), 126.8 ($C_4$ and $C_5$), 133.2 ($C_{8a}$ and $C_{9a}$), 133.4 ($C_3$ and $C_6$), 135.0 ($C_{4a}$ and $C_{5a}$), 141.1 ($C_2$ and $C_7$), 181.4 (C=O), 181.8 (C=O). EM $m/z$ (%) = 365 (33), 337 (7), 309 (10), 230 (13), 150 (85).

### 5.2. 1,8-Dibromo-10-anthrone 5

Sodium borohydride (8.26 g, 218.40 mmol) was added, portionwise, over 15 min to a stirred suspension of 1,8-dibromoanthraquinone **4** (10 g, 27.32 mmol) in methanol (300 mL) at −78 °C. After the addition was complete, stirring was continued for 3 h and then concentrated hydrochloric acid (30 mL) was added. The reaction mixture was heated at reflux overnight and then the yellow precipitate, which formed was collected, washed with water and dried to give a 7:3 mixture (as estimated by GC–MS) of anthrone **5** and quinone **4**. Compound **5** was purified by flash chromatography on silica gel with hexane (6.5 g, 68%). Mp: 264–267 °C. IR $\nu = 2961$, 2918, 2850, 1923, 1737, 1454, 1433, 1259 $cm^{-1}$. $^1H$ NMR (500 MHz, $CDCl_3$, 298 K): $\delta = 4.19$ (s, 2H, $H_9$ and $H_{9'}$), 7.38 (dd, $J = 7.9$ Hz, $J = 7.9$ Hz, 2H, $H_3$ and $H_6$), 7.89 (dd, $J = 7.6$ Hz, $J = 1.3$ Hz, 2H, $H_2$ and $H_7$), 8.33 (dd, $J = 7.6$ Hz, $J = 1.2$ Hz, 2H, $H_4$ and $H_5$). $^{13}C$ NMR (125 MHz, $CDCl_3$, 298 K): $\delta = 35.3$ ($C_9$), 124.7 ($C_{4a}$ and $C_{5a}$), 127.1 ($C_4$ and $C_5$), 128.5 ($C_2$ and $C_7$), 132.9 ($C_1$ and $C_8$), 137.1 ($C_3$ and $C_6$), 139.0 ($C_{8a}$ and $C_{9a}$), 182.9 (C=O). EM $m/z$ (%) = 352 (8), 351 (48), 272 (63), 244 (10), 193 (2), 163 (100).

### 5.3. 1,8-Dibromoanthracene 6

A 7:3 mixture of 1,8-dibromoanthrone **5** and 1,8-dibromoanthraquinone **4** (9.8 g, 19.1 mmol of **5** and 8.2 mmol of **4**) was suspended in diglyme (200 mL). The mixture was stirred and flushed with nitrogen for 15 min. $NaBH_4$ (4.21 g, 113.3 mmol) was added and after 2.5 h, methanol (52 mL) was added followed by another portion of $NaBH_4$ (1.9 g, 50.2 mmol). The orange solution was stirred at room temperature overnight and then glacial acetic acid added to bring the pH to 3–4, followed by concentrated HCl to pH < 2. After stirring at room temperature for 3 h, water was added and the resulting yellow precipitate collected, washed with water and dried. The yellow residue obtained was purified by flash chromatography on silica gel (hexane 100%) to provide 1,8-dibromoanthracene **6** (6.6 g, 69.5% with respect to 1,8-dibromoanthraquinone **4**). Mp: 168–170 °C. IR $\nu = 2922$, 2851, 1665, 1611, 1432, 1338, 1302 $cm^{-1}$. $^1H$ NMR (500 MHz, $CDCl_3$, 298 K): $\delta = 7.32$ (dd, $J = 8.5$ Hz, $J = 7.0$ Hz, 2H, $H_3$ and $H_6$), 7.83 (dd, $J = 7.0$ Hz, $J = 0.9$ Hz, 2H, $H_2$ and $H_7$), 7.97 (dd, $J = 8.5$ Hz, $J = 0.6$ Hz, 2H, $H_4$ and $H_5$), 8.42 (s, 1H, $H_{10}$), 9.19 (s, 1H, $H_9$). $^{13}C$ NMR (125 MHz, $CDCl_3$, 298 K): $\delta = 123.8$ ($C_{4a}$ and $C_{5a}$), 126.6 ($C_3$ and $C_6$), 127.1 ($C_9$), 128.3 ($C_{10}$), 128.4 ($C_4$ and $C_5$), 130.4 ($C_2$ and $C_7$), 131.2 ($C_{8a}$ and $C_{9a}$), 133.1 ($C_1$ and $C_8$). EM $m/z$ (%) = 336 (16), 335 (85), 257 (16), 176 (100).

### 5.4. 1,8-Trifluoroacetylanthracene 7

A solution (2.5 M) of butyllithium in hexane (11.9 mL, 29.8 mmol) was slowly added to an anhydrous diethyl ether (50 mL) solution of 1,8-dibromoanthracene (4 g, 11.9 mmol) kept under $N_2$ with continuous stirring and at 0 °C. The reaction was completed after 45 min. Then the mixture was cooled to −78 °C and an excess of trifluoroacetic anhydride was added dropwise (20.3 mL, 143 mmol). After 3 h, the trifluoroacetic anhydride was distilled and the solid residue was purified by flash chromatography on silica gel (hexane/dichloromethane 95/5 v/v) to give diketone **7** (2.30 g, 52%). Mp: 168–170 °C. IR $\nu = 2961$, 2931, 2871, 1703, 1554, 1542, 1174 $cm^{-1}$. $^1H$ NMR (500 MHz, $CDCl_3$, 298 K): $\delta = 7.64$ (dd, $J = 7.9$ Hz, $J = 7.9$ Hz, 2H, $H_3$ and $H_6$), 8.33 (m, 4H, $H_2$, $H_7$, $H_4$ and $H_5$), 8.58 (s, 1H, $H_{10}$), 10.6 (s, 1H, $H_9$). $^{13}C$ NMR ($CDCl_3$, 298 K): $\delta = 116.4$ (q, $^1J_{CF} = 467.7$ Hz, 2C, $CF_3$), 123.3 ($C_9$), 124.4 ($C_3$ and $C_6$), 126.8 ($C_{4a}$ and $C_{5a}$), 128.8 ($C_{10}$), 129.7 ($C_{8a}$ and $C_{9a}$), 131.5 ($C_1$ and $C_8$), 133.6 ($C_2$ and $C_7$), 136.1 ($C_4$ and $C_5$). EM $m/z$ (%) = 369 (58), 300 (100), 273 (44), 204 (46), 176 (45).

1-Trifluoroacetylanthracene **8** was also isolated (0.80 g, 24%). Subl. 115–116 °C. IR $\nu = 3056$, 2930, 2859, 1698, 1614, 1535, 1173, 1132 $cm^{-1}$. $^1H$ NMR (500 MHz, $CDCl_3$, 298 K): $\delta = 7.51$ (dd, $J = 8.5$ Hz,

$J = 7.3$ Hz, 1H, $H_3$), 7.55 (m, 2H, $H_6$ and $H_7$), 8.00 (m, 1H, $H_5$), 8.07 (m, 1H, $H_8$), 8.26 (d, $J = 7.2$ Hz, 1H, $H_4$), 8.29 (d, $J = 8.4$ Hz, 1H, $H_2$), 8.46 (s, 1H, $H_{10}$), 9.54 (s, 1H, $H_9$). $^{13}$C NMR (125 MHz, $CDCl_3$, 298 K): $\delta = 123.1$ ($C_3$), 125.1 ($C_9$), 125.9 ($C_1$ or $C_{4a}$), 126.7 ($C_7$), 126.7 (q, $^1J_{CF} = 121.6$ Hz, 2C, $CF_3$) 126.8 ($C_6$), 127.8 ($C_{9a}$), 127.9 ($C_{10}$), 127.9 ($C_5$), 129.2 ($C_8$), 131.6 ($C_{4a}$ or $C_1$), 131.8 ($C_{5a}$), 133.5 ($C_4$), 133.7 ($C_{8a}$), 137.3 ($C_2$), 181.9 (q, $^2J_{CF} = 33.2$ Hz, 2C, C=O). EM $m/z$ (%) = 274 (24), 205 (28), 179 (100), 177 (36).

### 5.5. α,α′-Bis(trifluoromethyl)-1,8-anthracenedimethanol 2

Sodium borohydride (25 mg, 0.661 mmol) was added to a solution of 1,8-trifluoroacetylanthracene **7** (128 mg, 0.346 mmol) in diethyl ether (25 mL). After 5 min of stirring, methanol (14 mL ca.) was added dropwise until the bubbling stopped. After 4.5 h the reduction was completed. The reaction was quenched and the crude was washed with water ($3 \times 25$ mL), the organic layer was separated, dried and concentrated. The solid residue (mixture of isomers) was purified by flash chromatography on silica gel (dichloromethane/hexane 95/5 v/v) to provide a pale yellow solid (119 mg, 92%).

### 5.6. (*R*,*R*)-α,α′-Bis(trifluoromethyl)-1,8-anthracenedimethanol (*R*,*R*)-2

A 1 M solution of (*S*)-methyl oxazaborolidine in toluene (0.65 mL, 0.65 mmol) was added to a solution of 1,8-trifluoroacetylanthracene **7** (288 mg, 0.78 mmol) in anhydrous toluene (10 mL) kept under nitrogen with continuous stirring. The mixture was cooled to −78 °C and a 1 M solution of catecholborane in toluene (4.0 mL, 4.0 mmol) slowly added (15 min). The reaction was stirred at −78 °C for 3 h and then left to warm to room temperature with stirring overnight. The reaction was quenched and the mixture was washed in water ($2 \times 20$ mL), a solution of 10% NaOH ($2 \times 20$ mL), HCl 1 M ($1 \times 20$ mL), water ($2 \times 20$ mL) and a solution of 10% $NaHCO_3$ ($2 \times 20$ mL). The organic layer was separated, dried and concentrated. Purification of the solid residue by flash chromatography on silica gel (dichloromethane 100%) provided 260 mg (89%) of compound (*R*,*R*)-**2**. $[\alpha]^{25} = -8.2$ (*c* 2, MeOH). Mp: 175–176 °C. IR $\nu = 3396$, 1259, 1154, 1122 cm$^{-1}$. $^1$H NMR (500 MHz, $CDCl_3$, 298 K): $\delta = 2.92$ (s, 2H, OH), 5.96 (q, $J =$ Hz, 2H, $H_{11}$), 7.52 (dd, $J = 8.6$ Hz, $J = 6.8$ Hz, 2H, $H_3$ and $H_6$), 7.82 (d, $J = 6.8$ Hz, 2H, $H_2$ and $H_7$), 8.05 (d, $J = 8.6$ Hz, 2H, $H_4$ and $H_5$), 8.51 (s, 1H, $H_{10}$), 8.96 (s, 1H, $H_9$). $^{13}$C NMR ($CDCl_3$, 298 K) $\delta$ (ppm): 70.5 ($C_{11}$), 118.4 ($C_9$), 125.0 (q, $CF_3$, $^1J_{C/F} = 122$ Hz), 125.3 ($C_3$ and $C_6$), 127.2 ($C_2$ and $C_7$), 128.9 ($C_{10}$), 129.7 ($C_{4a}$ and $C_{5a}$), 130.5 ($C_{8a}$ and $C_{9a}$), 130.7 ($C_4$ and $C_5$), 131.9 ($C_1$ and $C_8$). EM $m/z$ (%) = 374 (84), 355 (4), 305 (1), 287 (100), 178 (44). Anal. Calcd for $C_{18}H_{12}F_6O_2$: C, 57.76; H, 3.23. Found: C, 57.49; H, 3.49.

By using the same procedure but with (*R*)-methyl oxazaborolidine, compound (*S*,*S*)-**2** was obtained. $[\alpha]^{25} = +8.0$ (*c* 2, MeOH).

### 5.7. α,α′-Bis(trifluoromethyl)-1,8-anthracenedimethyl diacetate 9

Dimethylaminopyridine (DMAP) (12.4 mg, 0.102 mmol), triethylamine (358.5 mg 3.55 mmol) and acetyl chloride (200.0 mg, 2.55 mmol) were added to a solution of alcohol **2** (mixture of isomers) (95 mg, 0.254 mmol in 15 mL of anhydrous dichloromethane). After 3 h, the reaction had finished and the mixture was washed in water ($2 \times 20$ mL), HCl 1 M ($2 \times 20$ mL) and a solution of 10% $NaHCO_3$ ($2 \times 20$ mL). The organic layer was separated, dried and evaporated and 113 mg (97%) of compound **9** obtained. Mp: 160–162 °C. IR $\nu = 3020$, 1768, 1270, 1212–1124 cm$^{-1}$. $^1$H NMR (500 MHz, $CDCl_3$, 298 K): $\delta$ (ppm): 2.25 (s, 3H, $CH_3$), 7.05 (q, $J = 6.8$ Hz, 2H, $H_{11}$), 7.51 (dd, $J = 7.0$ Hz, $J = 7.0$ Hz, 2H, $H_3$ and $H_6$), 7.74 (d, $J = 7.0$ Hz, 2H, $H_2$ and $H_7$), 8.07 (d, $J = 8.5$ Hz, 2H, $H_4$ and $H_5$), 8.52 (s, 1H, $H_{10}$), 9.22 (s, 1H, $H_9$). $^{13}$C NMR (125 MHz, $CDCl_3$, 298 K): $\delta = 20.5$ ($CH_3$), 70.2 ($C_{11}$), 119.0 ($C_9$), 124.8 ($C_3$ and $C_6$), 128.3 ($C_2$ and $C_7$), 128.5 ($C_{10}$), 130.8 ($C_4$ and $C_5$), 168.9 (C=O).

Similar reaction was carried out from pure enantiomers (*R*,*R*)-**2** and (*S*,*S*)-**2** obtaining (*R*,*R*)-**9**. $[\alpha]^{25} = -8.2$ (*c* 2, MeOH) and (*S*,*S*)-**9**. $[\alpha]^{25} = +8.2$ (*c* 2, MeOH) in similar yield.

## Acknowledgements

Financial support from CICYT (BQU2003-01231) and predoctoral UAB grant to M.P-T. is gratefully acknowledged. V. Jimenez from University of Concepción, Chile, is also acknowledged.

## References

1. (a) Parker, D. *Chem. Rev.* **1991**, *91*, 1441–1457; (b) Wenzel, T. J.; Wilcox, J. D. *Chirality* **2003**, *15*, 256–270.
2. Pedras, M. S. C.; Hossain, M.; Sarwar, M. G.; Montaut, S. *Bioorg. Med. Chem. Lett.* **2004**, *14*, 5469–5471.
3. Pirkle, W. H. *J. Am. Chem. Soc.* **1966**, *88*, 1837.
4. Iuliano, A.; Bartalucci, D.; Ucello-Barretta, G.; Balzano, F.; Salvadori, P. *Eur. J. Org. Chem.* **2001**, 2177–2184.
5. Ucello-Barretta, G.; Mirabella, F.; Balzano, F.; Salvadori, P. *Tetrahedron: Asymmetry* **2003**, *14*, 1511–1516.
6. (a) Czerwenka, C.; Zhang, M.; Kählig, H.; Maier, N. M.; Lipkowitz, K. B.; Lindner, W. *J. Org. Chem.* **2003**, *68*, 8315–8327; (b) Shapiro, M. J.; Archinal, A. E.; Jarema, M. A. *J. Am. Chem. Soc.* **1989**, *54*, 5826–5828.
7. Narumi, F.; Hattori, T.; Matsumura, N.; Onodera, T.; Katagiri, H.; Kabuto, C.; Kameyama, H.; Miyano, S. *Tetrahedron* **2004**, *60*, 7827–7833.
8. (a) Rekharsky, M.; Yamamura, H.; Kawai, M.; Inoue, Y. *J. Am. Chem. Soc.* **2001**, *123*, 5360–5361; (b) Wenzel, T. J.; Amonoo, E. P.; Shariff, S. S.; Aniagyei, S. E. *Tetrahedron: Asymmetry* **2003**, *14*, 3099–3104; (c) Dodziuk, H.; Kozminski, W.; Ejecart, A. *Chirality* **2004**, *16*, 90–105.
9. (a) Lesot, P.; Lafon, O.; Courtieu, J.; Berdague, P. *Chem. Eur. J.* **2004**, *10*, 3741–3746; (b) Aroulanda, C.; Merlet, D.; Courtieu, J.; Lesot, P. *J. Am. Chem. Soc.* **2001**, *123*, 12059–12066.

10. Kobzar, K.; Kessler, H.; Luy, B. *Angew. Chem., Int. Ed.* **2005**, *44*, 3145–3147.
11. Seco, J. M.; Quiñoá, E.; Riguera, R. *Chem. Rev.* **2004**, *104*, 17–117.
12. Pirkle, W. H.; Muntz, R. L.; Paul, I. C. *J. Am. Chem. Soc.* **1971**, *11*, 2817–2819.
13. Pazos, Y.; Leiro, V.; Seco, J. M.; Quínoa, E.; Riguera, R. *Tetrahedron: Asymmetry* **2004**, *15*, 1825–1829.
14. Kobayashi, Y.; Hayashi, N.; Kishi, Y. *Org. Lett.* **2002**, *4*, 411–414.
15. Pomares, M.; Sánchez-Ferrando, F.; Virgili, A.; Alvarez-Larena, A.; Piniella, J. F. *J. Org. Chem.* **2002**, *67*, 753–758.
16. Comelles, J.; Estivill, C.; Moreno-Mañas, M.; Virgili, A.; Vallribera, A. *Tetrahedron* **2004**, *60*, 11541–11546.
17. Benites, M. R.; Fronczek, F. R.; Hammer, R. P.; Maverick, A. W. *Inorg. Chem.* **1997**, *36*, 5826–5831.
18. Marquardt, D. J.; McCormick, F. A. *Tetrahedron Lett.* **1994**, *35*, 1131–1134.
19. Haenel, M. W.; Jakubik, D.; Krueger, C.; Betz, P. *Chem. Ber.* **1991**, *124*, 333–336.
20. Lovell, J. M.; Joule, J. A. *Synth. Commun.* **1997**, *27*, 1209–1215.
21. Casarini, D.; Lunazzi, L.; Macciantelli, D. *J. Chem. Soc., Perkin Trans. 2* **1992**, 1363–1370.
22. Corey, E. J.; Helal, C. J. *Angew. Chem., Int. Ed.* **1998**, *37*, 1986–2012.
23. Estivill, C.; Ivanov, P. M.; Pomares, M.; Sanchez-Arís, M.; Virgili, A. *Tetrahedron: Asymmetry* **2004**, *15*, 1431–1436.
24. The crystal structure (−)-(*R*,*R*)-**2** has been deposited at the Cambridge Crystallographic Data Centre and allocated the deposition number CCDC 258683.
25. (a) Mohamadi, F.; Richards, N. G. J.; Guida, W. C.; Liskamp, R.; Caufield, C.; Chang, G.; Hendrickson, T.; Still, W. C. *J. Comput. Chem.* **1990**, *11*, 440–467; (b) MacroModel/BatchMin, v. 5; Department of Chemistry, Columbia University, New York, 1995.
26. The AMBER* force field is a well-documented version of AMBER force field, implemented in MacroModel/BatchMin, v.5 (see pp 81–82 of the BatchMin Reference Manual).
27. Job, P. *Ann. Chim.* **1928**, *9*, 113–203.
28. Fielding, L. *Tetrahedron* **2000**, *56*, 6151–6170.
29. Bouquant, J.; Chuche, J. *Tetrahedron Lett.* **1972**, *13*, 2337–2340.
30. Raber, D. J.; Hardee, L. E. *Org. Magn. Reson.* **1982**, *20*, 125–132.
31. Weber, G.; Anderson, S. R. *Biochemistry* **1965**, *4*, 1942–1947.
32. Koy, C.; Michalic, M.; Döbler, C.; Oehme, G. *J. Prakt. Chem.* **1997**, *339*, 660–663.
33. Stott, K.; Stonehouse, J.; Keeler, J.; Hwang, T. L.; Shaka, A. J. *J. Am. Chem. Soc.* **1995**, *117*, 4199–4200.